Patch-Clamp Measurements Reveal Multimodal Distribution of Granule Sizes in Rat Mast Cells

Guillermo Alvarez de Toledo and Julio M. Fernandez

Department of Physiology and Biophysics, Mayo Clinic, Rochester, Minnesota 55905

Abstract. Using patch-clamp techniques, we have followed the attributes of the secretory granules of peritoneal mast cells obtained from rats of different ages. The granule attributes were determined by following the step increases in the cell surface membrane area caused by the exocytosis of the granules in GTPγS stimulated mast cells. Our data show that the amount of granule membrane available for exocytosis depends exponentially on the weight (age) of the donor rat, reaching a maximum at ~300 g. The data are consistent with an exponential growth in the number of granules contained by mast cells of maturing animals. Histograms of the sizes of the step increases in surface area caused by exocytosis of the granules showed at least four equally spaced peaks of similar variance where the position of the first peak and the spacing between peaks averaged 1.3 ± 0.4 μm^2. In all cells recorded, no more than seven peaks could be found, the higher order peaks having a lower probability of occurrence. The distribution of granule sizes did not change measurably between young and adult animals. This study suggests that at least two separate steps may determine the size of a secretory granule: granule to granule fusion that may account for the subunit composition of granule sizes and traffic of microvesicles through the maturing granules that may account for the variance observed in the granule sizes. This study also demonstrates a novel way to study granulogenesis in living cells.

ALTHOUGH much progress has been made in understanding the synthesis, traffic, and sorting of secretory proteins, little is known about the formation of their storage containers, the secretory granules. It is widely accepted that secretory granules are formed from vesicles budding from the trans Golgi cisternae (Farquhar and Palade, 1981; Kelly, 1985; Griffiths and Simons, 1986). It is not known, however, what mechanisms determine the size of the secretory granules. In view of the "frantic membrane pinching-off and fusing" of subcellular organelles (Kelly, 1985), it is likely that granule size is not only determined by the size of the initial Golgi-derived vesicle but also undergoes modifications during the maturation process. Two mechanisms that may regulate granule size have been described by several authors in different cell types: the coalescence of Golgi-derived vesicles that form the immature granules and their subsequent modification through the recycling of small vesicles (Farquhar and Palade, 1981; Dvorak et al., 1980; Zastrow and Castle, 1987; Komuro et al., 1987). The traffic of small vesicles is tightly associated with granule maturation and is eventually arrested as more mature secretory granules loose their ability to fuse with the small vesicles (Tooze and Tooze, 1986; Komuro et al., 1987). However, direct evidence for the mechanisms that control granule size is still lacking.

Most of the evidence for the various schemes of granulogenesis comes from electron micrographs of thin sections of secretory cells. These measurements have to be interpreted using morphometric techniques to give statistical guesses of the number and size of the secretory granules contained in a cell (Nadelhaft, 1973). In contrast with previous techniques, measurements of the cell membrane capacitance can determine rapidly and accurately the attributes of the granules in unfixed living cells (Neher and Marty, 1982; Fernandez et al., 1984; Zimmerberg et al., 1987; Breckenridge and Almers, 1987; Maruyama, 1988). Regardless of its size or shape, fusion of a secretory granule with the plasma membrane causes a step increase in the surface membrane area of the cell, causing an increase in the cell membrane capacitance proportional to the granule surface area. Thus, by measuring the cell membrane capacitance of a secretory cell during exocytosis, it is possible to determine the size and number of the secretory granules contained by the cell. In this work, we use a combination of patch-clamp and circuit analysis techniques to measure the capacitance of the cell membrane of rat peritoneal mast cells undergoing exocytosis (Fernandez et al., 1984). Our measurements show that the number of secretory vesicles contained by a mast cell increases exponentially with the weight (age) of the donor rodent reaching a maximum at ~300 g corresponding to 8 wk after birth. We also show that the size of the granule membrane appears as an integral multiple of a basic unitary size that remains constant through granulogenesis. We interpret these results in relation to possible schemes of secretory granule formation.

Materials and Methods

Mast Cell Collection

Peritoneal mast cells were obtained from Sprague Dawley rats of various ages. The animals were classified by weight instead of age because of frequent uncertainties in their birthdates. There is, however, a close correlation between weight and age up to ~12 wk after birth. To extract mast cells, 5–50 ml of culture saline solution (see below) was injected into the peritoneal cavity of the rats. After some gentle massage of the rat's abdomen, the peritoneal cavity was surgically exposed, and 1–5 ml of fluid was recovered. The peritoneal wash fluid contained large numbers of cells, a small fraction of which were mast cells. Subsequently, the cell suspension was centrifuged at low speed (500 rpm) until a small white pellet formed at the bottom of the centrifugation tube. The pellet was then resuspended in ~1 ml of culture saline. This cell suspension was then seeded in the wells of our all-glass experimental chambers. The cells were then incubated at 37°C in a 5% CO_2 + 95% air atmosphere for ~30 min before use.

Solutions

The intracellular saline was composed of 140 mM K-glutamate, 7 mM $MgCl_2$, 10 mM Hepes, and 3 mM KOH. This solution was frozen and kept at −20°C in 10 ml aliquots until use. For the experiments, the solutions were thawed, and 200 μM Na_2ATP, 20 μM GTPγS (Sigma Chemical Co., St. Louis, MO), and 400 μM EGTA were added from separate frozen aliquots. The intracellular saline was adjusted to pH 7.2 and 290 mmol/kg. The extracellular saline was composed of 150 mM NaCl, 10 mM Hepes, 2.8 mM KOH, 1.5 mM NaOH, 1 mM $MgCl_2$, and 2 mM $CaCl_2$. The extracellular saline was adjusted to pH 7.2 and ~6 mM glucose was added to reach 300–310 mmol/kg. The culture saline consisted of extracellular saline plus 45 mM $NaHCO_3$ and 0.4 mM phosphate buffer at pH 7.2. All recordings were made at room temperature.

Measurements of the Cell Membrane Surface Area

We use the proportionality that exists between the surface area of biological membranes and their electrical capacitance to determine the surface membrane area contributed by a secretory granule when it fuses with the plasma membrane. The specific capacitance of biological membranes is thought to be ~1 μF/cm² (Cole, 1972). A good correlation between the observed range of sizes of secretory granules and their membrane capacitance has confirmed this value for the specific capacitance of the membrane of the secretory granules of rat mast cells (Fernandez et al., 1984). Throughout this work, we will assume that the specific capacitance of the membrane of the secretory granules and of the plasma membrane are equal to 1 μF/cm². This implies that a measured capacitance of 10 femtoFarads is equivalent to a membrane area of 1 μm².

We measure the cell membrane capacitance of perfused, voltage-clamped mast cells using a software based phase detector as described before (Joshi and Fernandez, 1988). In a few experiments, we have used also the more accurate procedures of phase tracking (Fidler and Fernandez, 1989). All recordings were done in the whole cell mode of the patch-clamp technique (Hamill et al., 1981). The reference electrode was a Ag/AgCl pellet connected to the extracellular medium via a 1 M KCl/Agar bridge. We measure current through the cell membrane at a phase angle ϕ with respect to the sinusoidal command voltage (50 mV, 833 Hz). We measure changes in the fraction of the total current that is measured at ϕ. These changes are proportional to the cell membrane capacitance. Both the phase angle ϕ and the proportionality factor are determined following the procedures described elsewhere (Joshi and Fernandez, 1988; Fidler and Fernandez, 1989). Every capacitance value is obtained by integrating eight sinusoidal cycles, generating one data point every 35 ms. The command input of the patch-clamp amplifier (EPC-7; List Electronics, Darmstadt, FRG) was controlled by the digital to analogue port of an Indec Systems Module interfaced either to a PDP11/73 (DEC) or AT clone (Beltron 286) computer. Data acquisition was done by the same computers. In a typical experiment, after establishing the whole cell recording mode, we applied a 10-mV square pulse of 1 ms duration to the command input of the patch-clamp amplifier. The resulting capacitive transient was canceled with the transient cancellation circuit of the EPC-7. When the transients were canceled, the impedances of the cell and of the compensation circuit were matched. Direct readout of the compensating values determined the initial capacitance of the cell. Phase detection was initiated after this initial adjustment. At this time a calibration of the capacitance trace was given by transiently unbalancing the compensating capacitance of the EPC-7 by exactly 100 fF. This calibrating signal was used as a reference throughout the experiment.

Results

Upon perfusing single rat peritoneal mast cells with patch-pipette solutions containing 20 μM GTPγS, the cell's surface membrane area expands as shown in Fig. 1. The initial surface membrane area of the cell becomes apparent (A_i) when the whole cell recording mode is established (Fig. 1, $t = 0$). Then after a lag period, the cell surface membrane area expands in a stepwise fashion to a final value A_f. The extent of the membrane expansion is represented as A_f/A_i. This large increase in the cell's surface membrane area is because of the fusion of all or the majority of the secretory granules contained in the cell (Fernandez et al., 1984; Breckenridge and Almers, 1987). We will use the expansion factor A_f/A_i as a measure of the total amount of granule membrane that the cell is able to release. Since the fusion of a secretory granule with the plasma membrane causes a step increase in surface membrane area by an amount equal to that of the granule membrane, the size of the step is a direct measure of the membrane area contributed by a single granule. Fig. 1 shows the expansion of the surface membrane to be composed of a sequence of steps of different amplitude, reflecting the fusion of individual granules. We characterize these events by their amplitude (A_i) and also by the latency (l_i) between steps.

Time Dependence of Granule Accumulation

We have found that the expansion factor A_f/A_i depends on the weight (age) of the donor animal. As shown in Fig. 2 *A*,

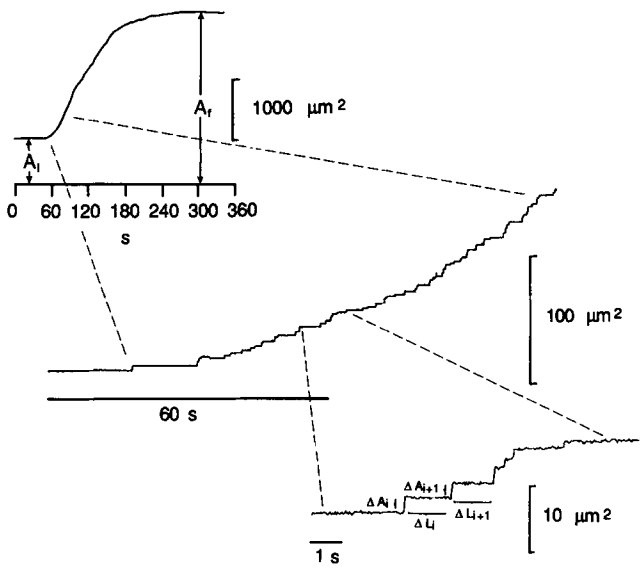

Figure 1. Characteristic expansion of the plasma membrane area caused by the exocytosis of secretory vesicles in rat peritoneal mast cells stimulated by intracellular perfusion with solutions containing 20 μM GTPγS. At the beginning of intracellular perfusion, we measure the initial surface membrane area (A_i). The surface membrane expands to a final value A_f. The ratio A_f/A_i reflects the total amount of membrane contained by the cell in the form of granules. The stepwise expansion of the plasma membrane marks the fusion of individual granules. These events are described by their amplitude A_i and the latency between events l_i.

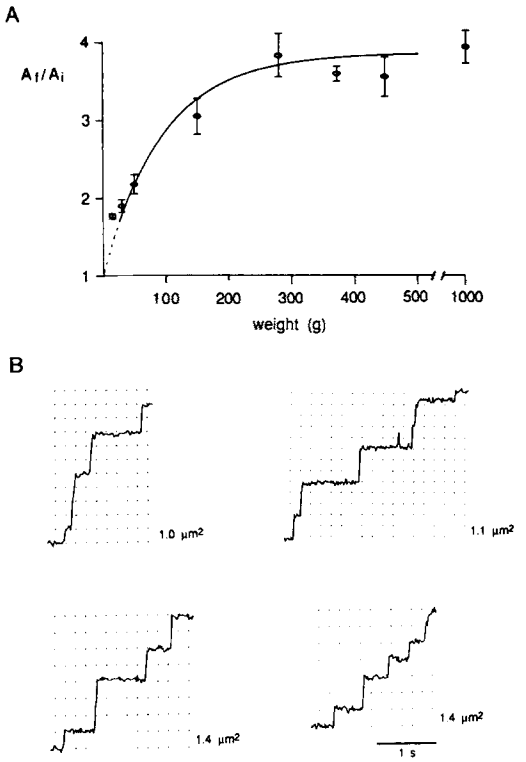

Figure 2. (*A*) Exponential dependency of the expansion factor A_f/A_i on the weight of the donor rodent. Note that 63% of the maximal attainable expansion is reached by animals weighing ~85 g corresponding to ~4 wk after birth. *B*, Periodic amplitudes of the step increases in surface membrane area caused by the fusion of single secretory vesicles. Results from four different cells showing that the amplitudes (A_i) of single fusion events appear as multiples of a basic unitary size (*dotted lines*). Note that the size of the unitary size may change from cell to cell.

the expansion factor ranges from $A_f/A_i = 1$ corresponding (hypothetically) to a cell where upon stimulation no measurable increase in capacitance is observed, to $A_f/A_i = 3.7$, the largest expansion factor observed. The solid curve corresponds to a single exponential with a weight constant of 85 g corresponding to ~4 wk after birth. In contrast to the expansion factor, the resting surface area of mast cells is relatively independent of the weight (age) of the donor animal (not shown).

Electron microscopic studies have shown that peritoneal mast cells obtained from newborn animals typically have very few secretory granules. In the course of ~8 wk after birth of the animal, mast cells fill with granules until they acquire their mature ultrastructural appearance with the cytoplasm densely packed with several layers of secretory granules. Mast cells release the majority or all their secretory granules when stimulated with guanine nucleotides (Fernandez et al., 1984); therefore our experimental results are consistent with the expansion factor A_f/A_i being a direct measure of the total amount of secretory granule membrane that the cell had accumulated and made available for exocytosis (see Discussion).

The Size of the Granule Membrane

The step increases in surface membrane area shown in Fig. 1 measure the amount of granule membrane contributed by each fusion event. Simple inspection of these recordings show a striking, previously unnoticed feature: the size of every fusion event appears as a multiple of a basic unit size. Fig. 2 *b* shows recordings from four different cells. These events clearly illustrate the multiunit composition of the individual fusion events. We routinely observe fusion events with sizes up to four, and in some cases up to seven times the size of the unitary events observed.

It is possible that the observations of Fig. 2 *B* correspond to simple random variation, where the observed multiples arise from a limited sample size. To rule out this possibility, we have compiled amplitude histograms for a larger number of fusion events, measured from individual mast cells undergoing degranulation. If the size periodicity observed in the individual fusion events arises from subunits, increasing the sample number would average out random variations, enhancing the multiunit formations. We investigate these possibilities in Fig. 3. As shown in Fig. 2 *B*, the size of unitary events varies from cell to cell. Simple summation of events from different cells would then erase the size periodicity. Instead, we computed size histograms from single cell data (Fig. 3, *A* and *B*). These histograms showed multiple peaks with equal spacing, confirming the features shown in Fig. 2 *B*. The unit size was obtained from the position of the first peak (2.15 μm^2 for the data in Fig. 3 *A*, and 1.1 μm^2 for that of Fig. 3 *B*). The average size of the steps corresponding to the first peak of the distribution was 1.3 μm^2 (SD, 0.4 μm^2, $n = 6$). To increase the sample number even more, we summed histograms obtained from single cells by first normalizing each histogram by the magnitude of the unitary size. Using this procedure, we obtained the histogram of Fig. 3 *C*. Fig. 3 *C* shows a histogram of 427 fusion events obtained from the normalized histograms of six different cells. As Fig. 3 *C* shows, even as the number of events is increased, the basic observations of Fig. 2 *B* are confirmed. Our findings strongly suggest that the subunit structure of the fusion events is real and does not result from random variations in the size of the fusion events.

As we have shown in Fig. 2 *A*, the accumulation of granules is conspicuously dependent on the weight (age) of the donor rat. Since the peculiar shape of the amplitude distributions shown in Fig. 3 is likely to reflect steps involved in the formation of the secretory granules (see Discussion), we have attempted to find changes in the amplitude distribution as the cells mature. This was done by compiling step amplitude distributions from cells obtained from donor animals of two weight (age) groups: (*a*) young, defined as animals of up to 50 g equivalent to ~3 wk of age; (*b*) adults, corresponding to donor animals of >300 g equivalent to eight wk or older. Fig. 4 shows the result of these experiments. Fig. 4 *A* shows the amplitude distribution of 225 steps from five cells obtained from young animals. Mast cells obtained from young animals are actively forming granules (see Fig. 2 *A*) but have accumulated relatively few. In spite of the smaller number of observations, Fig. 4 *A* shows clearly at least the first two broad peaks in the distribution. The average size of the steps that correspond to the first peak (1 in Fig. 4 *A*) was 1.1 μm^2 (SD, 0.2 μm^2, $n = 5$ cells). Fig. 4 *B* shows the amplitude distribution of 410 steps measured from 8 cells obtained from adult rats. The figure shows an amplitude distribution similar to that of Fig. 3 *C*. The average size of the steps cor-

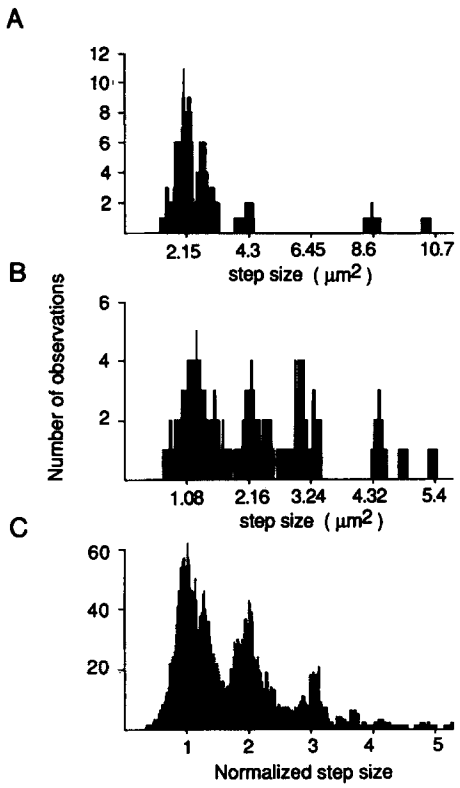

Figure 3. Amplitude distributions of step increases in surface membrane area A_i have regularly spaced peaks, confirming the data of Fig. 3 *B*. *A* and *B* show distributions of step sizes for individual cells. Note the varying amplitudes of each peak and also that the spacing of the peaks varies from cell to cell (2.15 μm^2 in *A* and 1.08 μm^2 in *B*). *C*, Amplitude distribution of 427 transitions obtained from six different cells obtained from donor animals of various weights (ages). The average magnitude of the first peak was 1.3 μm^2 (SD, 0.45 μm^2; $n = 6$). The data were pooled by normalizing single cell distributions by the estimated peak spacing. Note that the variance of the observed peaks does not change significantly from peak to peak. The relative height of the peaks, however, decreased with their order. The histograms shown were done using the moving bin technique with a bin size of 0.001.

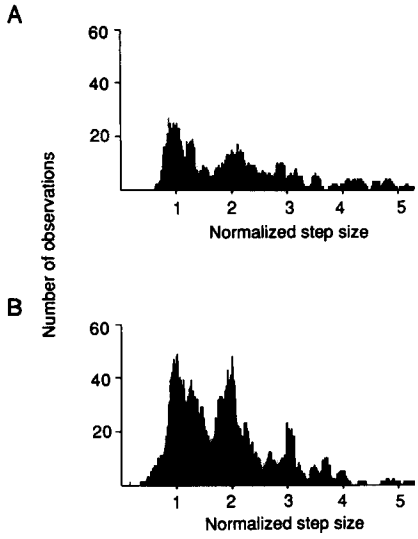

Figure 4. Amplitude distribution of step increases in surface membrane area A_i obtained from donor animals from different weight (age) groups. *A* shows the amplitude distribution of 225 steps recorded from five cells obtained from donor rodents ranging from 20 to 50 g (1–3 wk old). The average magnitude of the first peak was 1.1 μm^2 (SD, 0.2 μm^2, $n = 5$). *B* shows the amplitude distribution of 410 steps recorded from eight cells obtained from donor rodents weighing >300 g (older than 8 wk). The average magnitude of the first peak was 1.2 μm^2 (SD, 0.45 μm^2; $n = 8$). The histograms were done using the moving bin technique with a bin size of 0.001.

responding to the first peak of this distribution was 1.2 μm^2 (SD, 0.45 μm^2, $n = 8$ cells). As shown, the resulting distribution is not significantly different from that obtained from young rats or from the mixed distribution shown in Fig. 3 *C*. Although the proportion of bigger step sizes (i.e., second peak of distribution) seems to increase slightly with age, these changes are small. Thus, we conclude that the attributes displayed by the step amplitude distributions do not depend markedly on the weight (age) of the donor animal.

The Rate of Fusion of Secretory Granules

A simple explanation of the data in Figs. 2 *B*, 3, and 4 might be that because of our limited temporal resolution we observe superimposed, but independent, fusion events that are not time resolved. To explore this possibility, we estimated the probability of observing several independent fusion events within one sample period (see Materials and Methods) or 35 ms of each other. This probability can be obtained from the probability distribution of the latencies observed between fusion events. We define latency l_i as the time interval observed between fusion events (see Fig. 1). Fig. 5 (*inset*) shows a probability distribution histogram of the latencies between fusion events measured from a degranulating mast cell. This distribution $P(t)$ represents the probability of observing a second fusion event at a time longer than t seconds after observing the first one. The distribution function, $P(t) = \exp(-t/\tau)$, describes the data adequately (Fig. 5, *solid curve*; *inset*). Under our experimental conditions, two fusion

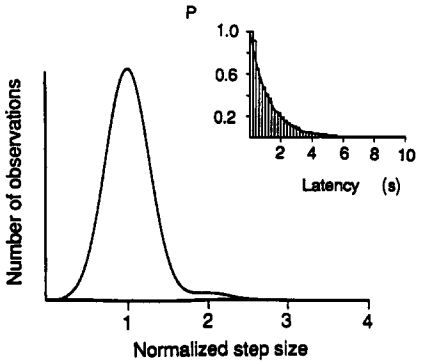

Figure 5. Computation of the probability of observing unresolved superimposed, but independent, fusion events. The proportion of superimposed events is calculated by using the probability distribution histogram of the latencies between exocytotic events l_i measured from the same data shown in Fig. 3 *B* (*inset*). An exponential fit (*solid curve*) adequately describes this function. Using this distribution, we can calculate the probability of observing two, three, or more events within one sample period of 35 ms.

events become indistinguishable from each other if they occur within 35 ms of each other (see Materials and Methods). By definition, the probability of finding a latency that is smaller or equal than 35 ms is $P(\leqslant 35 \text{ ms}) = 1 - P(>35 \text{ ms})$. We can calculate $P(\leqslant 35 \text{ ms})$ by using the value of τ obtained from the fits to the probability distribution data.

If a large number of exocytotic events is measured and if we assume that all the granules have normally distributed sizes with a mean value s_o and a variance σ, then because of the limited time resolution, a fraction of the events will superimpose and appear as larger multiples of their actual size. The measured distribution will then appear to have multiple peaks centered at $n \cdot s_o$. The relative amplitude of these peaks will be given by the relative magnitudes of $P^{n-1}(\leqslant 35$ ms). Finally, the variance of each peak should increase linearly with the order of the peak (i.e., as n).

Is it possible that an amplitude histogram showing multiple peaks can be entirely explained by the effect of a limited time resolution? For example, consider the amplitude histogram shown in Fig. 3 *B*. The probability distribution function of the latencies between the fusion events used to construct Fig. 3 *B*, is that shown in Fig. 5 (*inset*). Typically, these measurements are done at the beginning of the degranulation, where the rate of fusion is the fastest and does not change significantly. From the exponential fit to the data of Fig. 5 (*inset*), we measure tau = 1.2 s. Then, the probability of observing two superimposed fusion events would then be $P(\leqslant 35 \text{ ms}) = 0.013$, the probability of observing three superimposed fusion events would be $P^2(\leqslant 35 \text{ ms}) = 0.00017$ and so on. The predicted size distribution is shown in Fig. 5. As shown, this analysis predicts a small second peak and negligible higher order peaks. Clearly, the multiple peaks shown in Fig. 3 *C* cannot be due to superimposed events but rather to an endogenous process of granule formation. Similar results apply to all the data shown in Figs. 3 and 4. We cannot rule out, however, the existence of a fast process that synchronized the fusion of several granules simultaneously in packages in a way similar to that proposed for the action of the active zones of the neuromuscular junction. This hypothesis assumes that the secretory granules have, at rest, a size that corresponds to the size of the first peak in the size distributions. Electron microscopy of resting mast cells rules out this possibility. Measurements of the granule diameters observed in thin sections of resting mast cells predict sizes of secretory granule membrane areas ranging from 0.5 to 5 μm^2 (Fernandez et al., 1984). This wide range is sufficient to account for all the sizes observed not just the sizes of the first peak.

Discussion

Our results have demonstrated that in rat mast cells there is a close relationship between the degree of expansion of the plasma membrane upon complete degranulation and the body weight of the donor animal. Weight is considered a rough index of age (Padawer and Gordon, 1956). Since mast cell maturation is also well correlated with the age of the donor animal (Combs, 1966; Clausen et al., 1983), it seems logical to conclude that the weight dependent changes of the expansion factor A_f/A_i (Fig. 2 *A*) reflect mast cell maturation. As described in several reports, the most conspicuous aspect of mast cell maturation is the accumulation of the secretory granules (Combs, 1966; Clausen et al., 1983). Mast cells accumulate secretory granules for a period up to 8 wk after birth (Clausen et al., 1983). The majority, if not all, of the secretory granules formed during this period are simply accumulated in the cell without undergoing exocytosis (Padawer, 1974). Since we have shown (Fig. 4) that the granule size distribution does not change significantly with weight (age), it is likely that the weight dependent increase in the expansion factor A_f/A_i indicates the increase in the total number of granules contained by the cell as it matures. The good correlation between the time span of these changes and the length of the maturation period observed with EM (Clausen et al., 1983) also supports this conclusion.

Direct counting of the fusion events measured during a degranulation is the best way of determining the total number of secretory granules contained by a mast cell. Although Fig. 1 shows that we can easily resolve individual fusion events, it is only on rare occasions that we can resolve all the fusion events of a full degranulation. In most cases, large changes in the electrical equivalent circuit of the cell affect the quality of the recordings preventing us from observing all of the exocytotic events (Joshi and Fernandez, 1988). Under favorable conditions, we have been able to record up to two hundred events in a single cell. Mature mast cells, however, may have up to 1,000 or more secretory granules. In a typical experiment, we measure as many fusion events as possible, and then we measure the final surface area A_f of the cell membrane after degranulation is complete. This last measurement can be made very accurately (Joshi and Fernandez, 1988). Integration of a vesicle size distribution of the type shown in Figs. 3 and 4 gives the total contribution in surface membrane area that these vesicles would make if they all were to fuse with the plasma membrane of a single mast cell. It is possible to scale these distributions such that the total contribution of the vesicles matches the membrane expansion observed in any given cell, giving a realistic estimate of the number of secretory vesicles released. For example, if a mast cell expands from $\sim$600 μm^2 (resting surface membrane) to 960 μm^2 ($A_f/A_i = 1.6$) upon degranulation, this expansion can be explained by the fusion of 184 $\pm$ 55 ($n = 9$ cells) secretory granules whose sizes are distributed according to Figs. 3 and 4. Similarly, if the same cell had expanded fourfold to 2,400 μm^2, 789 $\pm$ 219 ($n = 9$ cells) secretory granules would be required.

The size of secretory granules cannot be measured directly from electron micrographs of thin sections because sectioning cuts any given granule at a random distance away from its center; thus, the observed diameters are not true diameters. The actual size distribution is generated by fitting the observed distribution with a model that takes into account the random sectioning (Nadelhaft, 1973). These estimates, however, rely heavily on the assumed geometry of the sectioned granules, typically assumed to be spherical. Mast cell granules are evidently nonspherical, compounding the problem of measuring their size. Not surprisingly then, electron microscope analysis of the cross-sectional areas of secretory granules from rat peritoneal mast cells, show broad and featureless distributions (Helander and Bloom, 1974; Hammel et al., 1983, 1988). Surprisingly, however, if the same data is represented as equivalent granule volumes, assuming that the granules are perfectly spherical, a multimodal distribution results (Hammel et al., 1983, 1988).

These data showed predicted granule volumes that were integral multiples of a unit volume of ~0.05 μm^3 (Hammel et al., 1983, 1988). If we assume that the granules are indeed perfect spheres, we calculate a corresponding surface area of ~0.68 μm^2. This value is smaller but close to the unitary fusion event observed with the patch-clamp technique (Figs. 2, 3, and 4). It is then possible that the granules with "unit volume," as predicted by the EM data may correspond to the fusion events of unit size, measured with the patch-clamp technique.

Although we have not determined the actual mechanisms responsible for the subunit composition of the granule fusion events, it is interesting to speculate on the possible implications that these observations may make to the biogenesis of the granules. Fig. 6 illustrates several possibilities.

The formation and packaging of secretory granules is an established function of the Golgi complex (Farquhar and Palade, 1981). In the early stages of formation, the granules appear continuous with the exit compartment of the Golgi complex; the trans Golgi network. In more mature stages, they detach and accumulate in the cytoplasm (Tooze and Tooze, 1986). It is possible that the membrane area of the secretory granules is determined at the time when they bud off the trans Golgi. This simple possibility is shown in Fig. 6 *A*. If this was true, then the characteristic distribution of granule sizes shown throughout this work would perhaps indicate restrictions and rules of assembly that pertain to the Golgi network.

It has been suggested that small Golgi-derived granules aggregate to form mature secretory granules (Farquhar and Palade, 1981). If the multiple sizes of the secretory granules resulted from the fusion of Golgi-derived granules, then we predict a diagram of events similar to that shown in Fig. 6*B*. Since the peak to peak noise of the capacitance measurements is <3 fF, corresponding to a total error of ~0.3 μm^2 in the membrane area of the granules, it is possible that the observed variance in the size of each peak results mainly from an actual variance in the size of the granule membrane. In this scheme, the size distribution of the Golgi-derived granules is similar in amplitude and variance to that of the first peak of the size histogram of Fig. 3 *C*. As the figure shows, fusion of such granules would create larger granules that are multiples of the Golgi-derived ones. However, since the variance of the sizes increases linearly with the order of the multiple (Boyd and Martin, 1956), higher order peaks are quickly diluted. In contrast, the data of Fig. 4 show that in spite of large changes in amplitude, the variance of the peaks of the size distribution does not change. A distribution of the type shown in Fig. 6 *B* describes the peaks in the amplitude of miniature end plate potentials resulting from the superimposition of quanta (Boyd and Martin, 1956).

Constitutive and regulated secretion appear to be related. Several authors have shown traffic of microvesicles between the plasma membrane and the membrane of maturing secretory granules in several cell types (Zastrow and Castle, 1987; Tooze and Tooze, 1986) including mast cells (Dvorak et al., 1980). This granule-associated traffic of microvesicles has been shown not to involve exocytosis of the granules themselves and may serve as a constitutive secretory mechanism (Zastrow and Castle, 1987). In rat somatotrophs labeled with cationized ferritin, it was observed that cationized ferritin accumulates in immature granules but not in mature

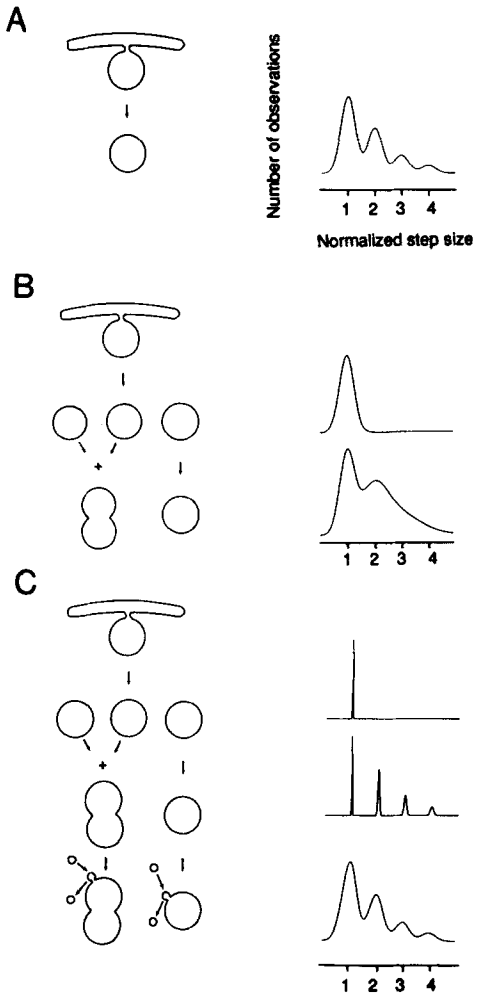

Figure 6. Hypothetical schemes that may explain the formation of secretory vesicles with their membranes being integral multiples of a unitary size. The left-hand diagrams show the various steps involved in the formation of the vesicles. The right-hand curves show the resulting amplitude histograms for each step. *A*, Secretory vesicles simply bud off the trans Golgi network having their final membrane area sizes without involving further steps. *B*, Unitary vesicles bud off the trans Golgi network with their sizes distributed according to the properties of the first experimentally observed peak. Subsequent fusion among the unitary vesicles produces multiple peaks in the size histogram. However, the variance increases linearly with the order of the peak resulting in a characteristic histogram where the peaks are blurred by the increasing variance. *C*, Unit granules bud off the trans Golgi network with little variance in their sizes. Subsequent fusion among unit granule forms multi-unit granules still showing little variance in their sizes. Traffic of microvesicles through the forming granules increases the variance of all the granule sizes. The origin of the microvesicles and the step at which microvesicles are incorporated into the granules is unknown. The microvesicle traffic have been included in the last stage of maturation only for the sake of clarity.

ones suggesting that the microvesicular traffic occurs mainly during granule maturation (Komuro et al., 1987). Furthermore it was frequently observed that immature granules had coated protuberances formed by microvesicles either fusing or pinching-off with the granule membrane. Komuro and collaborators proposed that as secretory granules mature,

they undergo a modification such that they lose their ability to fuse with the microvesicles. They also propose that these changes, that arrest the interactions between granules and microvesicles, may also determine the size of the mature granules (Komuro et al., 1987). The nature of the factors that control the ability of maturing granules to fuse among themselves, is unknown. However, since granule maturation appears linked with an increase in the density of the granule contents (Zastrow and Castle, 1987) it is conceivable that the same changes in the granule density arrest their fusion with the microvesicles. It is possible that these observations are a more general phenomena where maturing granules can fuse not only with microvesicles but also with themselves. Although most of these experiments have been done in different preparations and therefore may not be applicable to mast cells, we believe that these studies are particularly germane to our observations because they may provide an elegant explanation of our data: the secretory granule membrane would be the result of granule-to-granule fusion as well as fusion between granules and microvesicles. Fig. 6 *C* illustrates this hypothesis by showing the proposed stages involved in granule assembly. The initial step is the formation of granules with a well-defined unitary size. In contrast to the previous hypothesis (Fig. 6 *B*), these granules have little variance in the size of their membrane areas. A limited fusion among granules creates larger granules whose membrane areas are multiples of the unit size. Finally, traffic of microvesicles could be responsible for increasing the variance in the membrane surface area of all granules, by a similar amount. This increase in variance may be caused by a net difference in the number of microvesicles that fuse and pinch off from the maturing granules.

We thank Dr. Jonathan Monck for making valuable suggestions on the manuscript.

The research reported here was supported by the National Institutes of Health (grant GM-38857). Guillermo Alvarez de Toledo was supported by the Ministerio de Educación y Ciencia, Spain.

Received for publication 12 September 1989 and in revised form 16 November 1989.

References

Boyd, I. A., and A. R. Martin. 1956. The end-plate potential in mammalian muscle. *J. Physiol. (Lond.).* 132:74–91.

Breckenridge, L. J., and W. Almers. 1987. Final steps in exocytosis observed in a cell with giant secretory granules. *Proc. Natl. Acad. Sci. USA.* 84: 1945–1949.

Clausen, J., H. Jahn, and E. H. Nielsen. 1983. Electron microscopical study of rat mast cell maturation. *Virchows Arch. B Cell Pathol.* 43:151–158.

Cole, K. S. 1972. Membranes, Ions and Impulses. C. A. Tobias, Editor. University of California Press. 569 pp.

Combs, J. W. 1966. Maturation of rat mast cells. An electron microscope study. *J. Cell Biol.* 31:563–575.

Dvorak, A. M., M. E. Hammond, E. Morgan, N. S. Orenstein, S. J. Galli, and H. F. Dvorak. 1980. Evidence for a vesicular transport mechanism in guinea pig basophilic leukocytes. *Lab. Invest.* 42:263–276.

Farquhar, M. G., and G. E. Palade. 1981. The Golgi apparatus (complex)–(1954–1981)–from artifact to center stage. *J. Cell Biol.* 91(No. 3, Pt. 2):77s–103s.

Fernandez, J. M., E. Neher, and B. D. Gomperts. 1984. Capacitance measurements reveal stepwise fusion events in degranulating mast cells. *Nature (Lond.).* 312:453–455.

Fidler, N., and J. M. Fernandez. 1989. Phase tracking: an improved phase detection technique for cell membrane capacitance measurements. *Biophys. J.* 56:1153–1162.

Griffiths, G., and K. Simons. 1986. The trans Golgi network: sorting at the exit site of the Golgi complex. *Science (Wash. DC).* 234:438–443.

Hamill, O. P., A. Marty, E. Neher, B. Sakmann, and F. J. Sigworth. 1981. Improved patch-clamp techniques for high-resolution current recording from cells and cell-free membrane patches. *Pfluegers Arch. Eur. J. Physiol.* 391:85–100.

Hammel, I., D. Lagunoff, M. Bauza, and E. Chi. 1983. Periodic, multimodal distribution of granule volumes in mast cells. *Cell Tissue Res.* 228:51–59.

Hammel, I., D. Lagunoff, and P. G. Kruger. 1988. Studies on the growth of mast cells in rats. Changes in granule size between 1 and 6 months. *Lab. Invest.* 59:549–554.

Helander, H. F., and G. D. Bloom. 1974. Quantitative analysis of mast cell structure. *J. Microsc. Oxf.* 100:315–321.

Joshi, C., and J. M. Fernandez. 1988. Capacitance measurements: an analysis of the phase detector technique used to study exocytosis and endocytosis. *Biophys. J.* 53:885–892.

Kelly, R. B. 1985. Pathways of protein secretion in eukaryotes. *Science (Wash. DC).* 230:25–32.

Komuro, M., Y. Kiuchi, and T. Shioda. 1987. Membrane modification during secretory granule formation in rat somatotrophs. *Eur. J. Cell Biol.* 43: 98–103.

Maruyama, Y. 1988. Agonist-induced changes in cell membrane capacitance and conductance in dialysed pancreatic acinar cells of rats. *J. Physiol. (Lond.).* 406:299–313.

Neher, E., and A. Marty. 1982. Discrete changes of cell membrane capacitance observed under conditions of enhanced secretion in bovine adrenal chromaffin cells. *Proc. Natl. Acad. Sci. USA.* 79:6712–6716.

Nadelhaft, I. 1973. Measurement of the size distribution of zymogen granules from rat pancreas. *Biophys. J.* 13:1014–1029.

Padawer, J. 1974. Mast cells: extended lifespan and lack of granule turnover under normal in vivo conditions. *Exp. Mol. Pathol.* 20:269–280.

Padawer, J., and A. S. Gordon. 1956. Peritoneal fluid mast cells: their numbers and morphology in rats of various body weights (ages). *J. Gerontol.* 11: 268–272.

Tooze, J., and S. A. Tooze. 1986. Clathrin-coated vesicular transport of secretory proteins during the formation of ACTH-containing secretory granules in AtT20 cells. *J. Cell Biol.* 103:839–850.

Zastrow, M., and J. D. Castle. 1987. Protein sorting among two distinct export pathways occurs from the content of maturing exocrine storage granules. *J. Cell Biol.* 105:2675–2684.

Zimmerberg, J., M. Curran, F. S. Cohen, and M. Brodwick. 1987. Simultaneous electrical and optical measurements show that membrane fusion precedes secretory granule swelling during exocytosis of beige mouse mast cells. *Proc. Natl. Acad. Sci. USA.* 84:1585–1589.